Micro-PET imaging of angiogenesis based on 18F-RGD for assessment liver metastasis in colorectal cancer

Mingyu Zhang
Capital Medical University Affiliated Beijing Friendship Hospital
Hao Jiang
Second Affiliated Hospital of Harbin Medical University
Huijie Jiang (zmyjhj@163.com)
Second Affiliated Hospital of Harbin Medical University https://orcid.org/0000-0003-0658-8493
Rongjun Zhang
Jiangsu Institute of Nuclear Medicine
Zhenchang Wang
Capital Medical University Affiliated Beijing Friendship Hospital

Primary research

Keywords: RGD peptide, positron emission tomography, gastrointestinal cancer, metastasis

Posted Date: May 20th, 2020

DOI: https://doi.org/10.21203/rs.3.rs-29007/v1

Abstract

Background: This study aimed to explore the feasibility of 18 F-AlF-NOTA-E[PEG4-c(RGDfk)]2 (denoted as 18 F-RGD) PET quantitative parameters to distinguish the angiogenesis in colorectal cancer (CRC) mice which has different metastatic potential.

Methods: Animal models of CRC liver metastases were established by implanttation of human CRC cell lines LoVo and LS174T via intrasplenic injection. Radiotracer-based micro-positron emission tomography imaging of animal model was performed and the uptake of 18 F-RGD tracer in the tumor tissues were quantified as tumor-to-liver maximum or mean standardized uptake values ratio. Pearson correlation was used to analyze the relationship between radioactive parameters and tumor markers.

Results: The SUVmax ratio and SUVmean ratio of LoVo model was significantly higher than LS174T ones in both liver metastasis and primary tumor lesions ($P < 0.05$). A significantly difference was observed in both VEGF and Ki67 expression between LoVo and LS174T primary tumors ($P < 0.05$). The T/L SUVmean or SUVmax ratio of 18 F-RGD showed a significantly correlation with VEGF expression, but weakly correlated with Ki67 expression. The areas under the ROC curves of 18 F-RGD SUVmean ratio for differentiate LoVo from LS174T tumor was 0.801.

Conclusions: The T/L SUVmean ratio of 18 F-RGD is a promising parameters for tumor imaging and monitoring angiogenesis process in CRC xenograft mice model.

Introduction

Colorectal carcinoma (CRC) is the third most commonly diagnosed malignancy worldwide and liver metastasis is one of the main cause of CRC-related death[1, 2]. Tumor metastases is the culprit associated with cancer-related deaths, represent the end-products of cell-biological process[3]. Although the progression-free survival of multiple cancer has significantly increased profit from early detection and improved by individualized therapeutic regimens of modern clinical medicine, metastasis remains as the ultimate obstacle in our fight against cancer. A majority of CRC patients with liver metastasis face with poor prognosis and low overall survival rate.

The accumulation of tumor metastasis molecular mechanisms over the past decade has given us an in-depth understanding of the biological behavior of metastatic progression in various kinds of cancers[4]. Angiogenesis is defined as the formation of new blood vessels from the pre-existing microvasculature network. The supplement of neovascular is the key factor in malignant tumor growth, progression, and metastasis [5, 6]. The neovascularization in tumor is complex and disorganized. Vascular endothelial growth factor(VEGF)has been identified as the most important regulator of tumor angiogenesis, which widely expressed in a variety of tumors. The overexpressed VEGF in tumor cells or tumor microenvironment can promote CRC tumor growth and hematogenous metastasis by stimulating angiogenesis [7, 8]. Integrins are cell adhesion receptors for extracelluar matrix (ECM) proteins, and highly expressed on the surface of various cancer cells and neovascular endothelial cells. Tumor cells can

migrate effectively on ECM substrates, and the multiple integrin functioning contributes to this process and plays an important role in tumor angiogenesis. Among all integrins, integrin αvβ3 probably the most strongly involved in the regulation of angiogenesis[9]. The specifical interaction between integrin αvβ3 and vascular endothelial growth factor receptors (VEGFRs) is considered to be crucial for tumor growth and metastasis[10].

Positron emission tomography (PET) imaging is a non-invasively method to visualize and quantify the tumor microenvironment, such as proliferation and angiogenesis *et al*. Arginine-glycine-aspartic acid (RGD)-based peptides are well-known to specifically bind with integrin αvβ3 and considered to be a promising positron emission tomography (PET) tracer for monitoring the status of tumor angiogenesis[11]. However, there are few reports on the prediction of tumor metastasis potential based on assessment of tumor angiogenesis status. Therefore, in this study, we investigated the feasibility of dimeric RGD peptides-based PET quantitative parameters to distinguish the angiogenesis in CRC mice which showed different metastatic potential and to predict the metastatic potential of CRC in mice model. These findings may contribute to the better understanding neovascular microenvironment of CRC noninvasively and to yield useful radioactive markers, which are necessary to guide personalized therapeutic regimens.

Materials And Methods

Cell Culture

The human colorectal cancer cell lines LoVo and LS174T were purchased from the Type Culture Collection of the Chinese Academy of Sciences, Shanghai, China. LS174T cell line was derived from the primary lesion of colorectal adenocarcinoma, Dukes' type B; LoVo cell line was derived from the left supraclavicular metastatic site of colorectal adenocarcinoma, Dukes' type C. The LoVo and LS174T cell lines were maintained in Dulbecco's Modified Eagle Medium (DMEM, Gibco Corporation, USA) supplemented with 10% fetal bovine serum (Hyclone, USA) and 1% penicillin-streptomycin (Beyotime Biotechnology, China). All cells were cultured in a humidified atmosphere containing 5% CO_2 air at 37ºC.

Animal model

Five-week-old female BALA/C nude mice (weight, 16–18 g) were purchased from Animal Laboratory of Cavens Corporate of Changzhou (Changzhou, China). Colorectal cancer liver metastases (CLM) xenograft models were established by injecting LoVo or LS174T cells (2.0×10^7 cells in 0.15 mL of phosphate-buffered saline) into spleen which anesthetized by intraperitoneal injection of 10% chloral hydrate, respectively (n=20). All the animals were housed in an environment with temperature of 22 ± 1 ºC, relative humidity of 50 ± 1% and a light/dark cycle of 12/12 hr. All animal experiments were conducted in compliance with the protocols approved by the Institutional Animal Care and Use Committee (IACUC) of Jiangsu Institute of Nuclear Medicine. The body weight of nude mice was recorded every three days.

Radiopharmaceutical preparation

^{18}F-AIF-NOTA-E[PEG4-c(RGDfk)]2 (denoted as ^{18}F-RGD) was acquired by Jiangsu Key Laboratory of Molecular Nuclear Medicine, Jiangsu Institute of Nuclear Medicine. Synthesis of ^{18}F-RGD has been described previously [12]. ^{18}F-RGD was a glutamic acid linked dimeric RGD labeled with NOTA-^{18}F-AIF that has been proved to be safe and stable for PET imaging [11].

Cellular uptake *in vitro*

LoVo and LS174T cells were maintained in corresponding medium for 24 hours before ^{18}F-RGD cellular uptake. For normal group, the cells, ^{18}F-RGD and buffer (DMEM containing 0.2% bovine serum albumin) were mixed into a glass test tube (2ml). For block group, the cells, ^{18}F-RGD and inhibitor buffer were mixed into a glass test tube (2ml). All the glass test tube were incubated at 37°C for 1 hour. The tubes were divided in three groups: Group O was used as a control tube, composed of 100μl radionuclides and 200μl buffer (DMEM buffer with 0.2% BSA); Group T was used to measure the radionuclide dose, contained 100μl radionuclides; Group X, was composed of 100μl radionuclides, 100μl cell suspension and 100μl corresponding buffer. The cellular uptake was normalized to 5×10^5cells/tube; each cell line was tested three times at each time point. The radioactivity of each cell line at 1 hour was accurately measured using Automatic Gamma Counter (PerkinElmer, 2480, USA). The cellular uptake ratio was calculated using the following formula: *X(cpm)-0(cpm)/T(cpm)%*.

Micro-PET Imaging and analysis

^{18}F-RGD PET imaging of LoVo and LS174T-CLM mice models (n=20) were performed seven weeks after implantation. Six-minute static ^{18}F-RGD (About 9.25MBq, 250μCi) was acquired 1 hours (radiopharmaceutical administration time in mice) after injection via tail vein. All the mice were anesthetized with 2% isoflurane in 100% oxygen with a flow rate of 2 L/min prior to imaging. Micro-PET scans were acquired in 3-dimensional mode using an Inveon micro-PET scanner (Siemens Medical Solutions) with an ordered-subset expectation maximization/maximum: matrix, 128×128×159; pixel size, 0.86×0.86×0.8mm; β-value, 1.5, with uniform resolution. PET images were reconstructed and postprocessed using Inveon Acquisition Workplace software (version 2.0, Siemens Preclinical Solutions).

Regions of interests (ROIs) were drawn on images around the entire liver metastasis or primary tumor lesions and normal liver tissue using ASI Pro VM 6.8.6.9 software (Concorde Microsystems, LLC). The maximum/mean standardized uptake value (SUVmax/mean) ratio was calculated as the tumor-to-liver SUVmax/mean (T/L ratio). All Micro-PET imaging procedures were conducted according to protocol approved by the Jiangsu Institute of Nuclear Medicine Animal Care and Use Committee.

Immunohistochemical staining

The tumor specimens were fixed in 10% formalin for 48 h, paraffin-embedded, and cut into 3 μm-thick sections. Immunohistochemical staining was performed as previously described [13]. Briefly, the slides were incubated with anti-Ki67 (1:100, ab16667, Abcam) or anti-VEGF (1:200, ab46154, Abcam) at 4°C overnight. Next, the slides were incubated with horseradish peroxidase-labeled goat anti-mouse or anti-rabbit secondary antibody (Boster, Wuhan, China) at room temperature followed by counterstaining with hematoxylin. The staining was observed under a BX53 Olympus microscope (Olympus, Japan) at magnification 200×. A brown-yellow staining was defined as positive expression. Ki67 or VEGF protein were quantitated by Image-J software (NIH, Bethesda, MD, USA).

Statistical analysis

All data were expressed as mean±standard deviation. Statistical analyses were performed using R version 3.6.1 (www.R-project.org). The difference between two groups was assessed using Student's unpaired *t*-test. The Fisher exact test was used for comparing differences in liver metastatic potential *in vivo*. The correlation between the RGD parameters and tumor marker was analyzed using Pearson correlation analysis. The receiver operating characteristic (ROC) curve was used to differentiate LoVo tumor from LS174T tumor. A P value <0.05 was considered statistically significant.

Results

1. Comparison of metastatic potential and malignancy between the two models

Firstly, we calculated the tumor formation rate (including primary tumor and liver metastasis) of CLM model mice to evaluate the *in vivo* metastatic potential of LoVo and LS174T colorectal cancer cells (Table 1). Liver metastasis rate was defined as: the number of mice with liver metastasis divide by the number of mice with primary tumor in spleen. The liver metastasis rate of LoVo-CLM mice (66.67%) was significantly higher than LS174T ones (41.67%) (X^2 = 6.559, P = 0.039). In addition, the median survival time of LoVo and LS174T CLM models were 8 and 11.5 weeks respectively (P = 0.0006; Fig. 1A). The results show that LoVo-CLM mice has a shorter survival time compared to LS174T-CLM mice. In addition, the body weight of LoVo and LS174T CLM models shown in Fig. 1B also confirmed that LoVo cells demonstrated a higher metastatic potential than LS174T cells *in vivo*. Our next experiments will be based on these two cells with differences in metastatic potential.

Table 1
The liver metastasis rate of CRC models.

	The tumor incidence				
Cell line	The number of CLM models	Only primary tumor in spleen	Both liver metastasis and primary tumor	No tumor	Liver metastasis rate
LoVo	20	6	12	2	66.67%
LS174T	20	7	5	8	41.67%
X^2	6.559[a]				
P value	0.039				
$p<0.05$ is considered statistically significant					

2. *In vitro* cellular ^{18} F-RGD uptake analysis of LoVo and LS174T cell line

For uptake study, we detected the difference of ^{18}F-RGD cellular uptake between LoVo and LS174T cell lines in vitro. Our results showed that the cellular uptake of LoVo cell (3.07%±0.28) at 1 hour was higher than LS174T (2.43%±0.63) ones, unfortunately, there has no statistical significance (*P*0.05). Compared with the data of 1 h group, the cellular uptake of both LoVo (1.61%±0.04) and LS174T (0.88%±0.06) cells in 1 h block group were decreased significantly. These results indicate that LoVo and LS174T cells of colorectal cancer has a weak ^{18}F-RGD uptake *in vitro*, the uptake of ^{18}F-RGD depends on the microenvironment of solid tumors.

3. Comparison of ^{18}F-RGD parameters between LoVo and LS174T models

We next compared the difference of ^{18}F-RGD parameters between LoVo and LS174T CLM models *in vivo*. The ^{18}F-RGD parameters of liver metastasis and primary tumor were measured 1 h post ^{18}F-RGD injection. The liver metastasis tumor and primary tumor in spleen were confirmed by HE staining (Fig. 2A). The 6 minutes static scan of whole-body ^{18}F-RGD PET were performed in Fig. 2B. Our results showed that LoVo CLM model had a significantly higher SUVmean ratio and SUVmax ratio values in both liver metastasis and primary tumor than LS174T ones (P*<0.05*). The ^{18}F-RGD parameters of both SUVmean ratio and SUVmax ratio in primary tumor were higher than corresponding liver metastasis tumor (Table 2). Our results indicated that tumor with high metastasis potential prone to high ^{18}F-RGD uptake *in vivo*.

Table 2

The ^{18}F-RGD parameters in LoVo and LS174T CLM models

	Liver metastasis tumor			Primary tumor in spleen		
Cell line	N(liver metastasis)	SUVmean ratio	SUVmax ratio	N(primary tumor)	SUVmean ratio	SUVmax ratio
LoVo	12	1.38 ± 0.09	1.42 ± 0.08	18	1.55 ± 0.08	1.65 ± 0.11
LS174T	5	1.23 ± 0.06	1.26 ± 0.07	12	1.46 ± 0.05	1.55 ± 0.68
P value		0.03	0.001		0.004	0.01
$p<0.05$ is considered statistically significant						

4. Tumor markers of VEGF and Ki67 expression in LoVo and LS174T primary tumor

Since tumor markers VEGF and Ki67 are associated with tumor progress and metastasis, we next compared the heterogeneous staining of VEGF and Ki67 between LoVo and LS174T primary tumor in spleen. Immunohistochemical staining demonstrated that VEGF protein was mainly expressed in the cytoplasm and occasionally in the nucleus, whereas Ki67 protein was expressed in cell nucleus (Fig. 3A). Both VEGF and Ki67 expression in LoVo tumor were higher than that in LS174T tumor with a significant difference (P<*0.05*), as shown in Fig. 3B.

5. Correlation Analysis

We next investigated whether ^{18}F-RGD parameters can reflect the tumor angiogenesis or tumor proliferation *in vivo*. In Fig. 4, the results showed that no correlation was seen between RGD SUVmax ratio and Ki67 expression (P = 0.0718), however, a weak correlation was found between ^{18}F-RGD SUVmean ratio and Ki67 expression (P = 0.0438). On the contrary, the significant correlation was found between ^{18}F-RGD SUVmax ratio or SUVmean ratio and VEGF expression in primary tumor (P = 0.001 and P<0.0001, respectively). Our results demonstrated that the parameters of ^{18}F-RGD can reflect tumor angiogenesis.

6. Diagnostic performance of ^{18}F-RGD parameters to differentiate LoVo from LS174T tumors

Further, we investigated whether ^{18}F-RGD parameters in primary CRC can distinguish LoVo tumor from LS174T tumor, and can assess the tumor metastatic potential from the primary lesion. The ROC curve analysis were summarized in Table 3 and Fig. 5. The areas under the ROC curves (AUC) of ^{18}F-RGD

SUVmean ratio, SUVmax ratio and SUVmean ratio combined with SUVmax ratio for differentiate LoVo from LS174T tumor was 0.801, 0.759 and 0.787 respectively. The optimal cut-off value to differentiate LoVo from LS174T tumor was 1.551 for SUVmean ratio, 1.629 for SUVmax ratio and 0.759 for SUVmean ratio combined with SUVmax ratio. In addition, the sensitivity and specificity of SUVmean ratio to differentiate LoVo from LS174T tumors in mice models were 100% and 61.1%, respectively, the same as SUVmean combined with SUVmax ratio. Our results demonstrated that SUVmean ratio with a good AUC is a suitable parameter for predicting the metastatic potential of CRC in animal models.

Table 3

ROC curve analysis for ^{18}F-RGD parameters in LoVo and LS174T tumor

parameters	AUC	95%CI	P value	Optimal cut-off	Sensitivity	Specificity
SUVmean ratio	0.801	0.641–0.961	0.006	1.551	1.000	0.611
SUVmax ratio	0.759	0.584–0.934	0.008	1.629	0.917	0.611
SUVmean ratio + SUVmax ratio	0.787	0.618–0.956	0.007	0.759	1.000	0.611
$p<0.05$ is considered statistically significant						

Discussion

Tumor metastasis is the leading cause of CRC-related death. In patients with CRC metastasis, distant metastasis is usually confined to an isolated organ. Liver is the most common site of CRC metastasis [14]. Understanding the biological characteristics of tumor metastasis is the essential prerequisite for predicting CRC metastasis. Angiogenesis provides favorable conditions for tumor growth and metastasis,Folkman J *et al* suggested that tumors transformed into metastatic potential must undergo an “angiogenic switch” by perturbing the balance of proangiogenic and antiangiogenic factors [15]. Tumors with VEGF-overexpressed were more prone to occur “angiogenic switch”, consequently converting to metastatic potential.

In recent years, advances in the field of anti-angiogenesis therapy in oncology have provided more options for the treatment of cancer patients. More and more preclinical and clinical researches were focusing on how to monitor the tumor angiogenesis and treatment response by using multiple imaging modalities such as PET, SPECT, molecular MRI, targeted ultrasound, or optical imaging. Integrins are strongly involved in mediating adhesion events during tumor metastasis by activating many cellular signaling pathways, and the expression of integrin αvβ3 is mostly correlated with tumor metastatic potential[16, 17]. RGD peptides-based PET imaging for evaluation tumor angiogenesis and proliferation is a promising non-invasive method for understanding the tumor biological behavior [18]. In addition, integrin αvβ3 plays an important role in regulating tumor angiogenesis and proliferation. Our results

evidenced that a significant correlation between the 18F-RGD tracer parameters and VEGF expression in primary CRC tumor. Moreover, the SUVmean ratio of ^{18}F-RGD in primary tumor had the ability to distinguish LoVo tumor from LS174T tumor in mice model, which were with different tumor metastatic potential.

In this trail, we firstly compared the liver metastatic potential of LoVo and LS174T cells *in vivo* by establish a liver metastasis model. The results showed that LoVo-CLM models had a higher liver metastatic rate than LS174T ones (66.67% *vs* 41.67%), in addition, LoVo-CLM mice has a shorter survival time compared to LS174T-CLM mice (8 *vs* 11.5 weeks), suggesting that LoVo cells exhibited a stronger metastatic capability than LS174T ones. The result was same with our previous study[19].

The ^{18}F-RGD tracer was selected for assessing integrin αvβ3 expression and used its radiological parameters to quantify the angiogenesis of CRC in mice model. For the cellular uptake of ^{18}F-RGD *in vitro*, a low RGD uptake was found in two cells and there was no statistical difference between LoVo and LS174T cells at 1 h post-incubation. The reason for this phenomenon can be explained as an inactive or “off” state of integrins expressed on cell surfaces, in which they do not bind ligands and do not signal[20]. In order to explore the expression levels of integrins in solid tumor neovascularization of CRC mice, we perform ^{18}F-RGD PET imaging 1 hours post-injection and compare the radiological parameters between LoVo and LS174T mice. We delineated the ROI in liver metastases and primary splenic tumors according to corresponding anatomical locations. In further *in vivo* PET experiments, the encouraging data showed that the expression of integrin αvβ3 in tissue was superior to cells, and the parameters of ^{18}F-RGD SUVmean/SUVmax ratio was capable of distinguish the differences in angiogenesis between LoVo and LS174T mice. Integrin αvβ3 is mainly expressed on vascular endothelial cells,and therefore exhibits good ^{18}F-RGD uptake in tumor tissues with neovascular networks[21]. Our results demonstrated that tumors with high metastatic potential have high ^{18}F-RGD uptake capacity, acquisition of angiogenic properties accelerate the change from a quiescent to an invasive phenotype which known as “angiogenic switch”[22].

VEGF, which is an important factor in tumor angiogenesis, and Ki67, which is a nucleolar protein widely appreciated as a cell proliferation, are both associated with tumor growth and metastasis [23, 24]. Our quantification of immunohistochemical staining in primary tumor showed that the expression of VEGF and Ki67 in LoVo tissues were stronger than LS174T ones, combined with the results of correlation analysis, a weak correlation between ^{18}F-RGD SUVmean ratio and Ki67 expression ($P = 0.0438$) and a strongly significant correlation between RGD SUVmax ratio/SUVmean ratio and VEGF expression in primary tumor ($P = 0.001$ and P□0.0001, respectively), indicating that the SUVmax ratio/SUVmean ratio of ^{18}F-RGD may be recognized as an ideal radiation maker to reflect tumor angiogenesis in CLM mice model. Our viewpoint was consistent with previous reviews, that ^{18}F-RGD is a promising tracer for tumor angiogenesis imaging and monitoring anti-angiogenesis therapy in solid tumor[25, 26]. In Sibel Isal’s study, they also verified that the expression of integrin αvβ3, which are targeted by RGD-based peptides tracer, was associated with cell proliferation in glioblastoma [27].

We aimed in this study to predict tumor metastatic potential in primary CRC tumor using radiolabeled-RGD peptides. According to the ROC analysis, ^{18}F-RGD parameters of SUVmean ratio and SUVmax ratio has the capacity to distinguish LoVo tumor from LS174T tumor, among these SUVmean ratio shown the highest areas under the ROC curves (AUC) with the sensitivity 100% and specificity 61.1%. A SUVmean ratio of ≥ 1.551, a SUVmax ratio of ≥ 1.629 and a SUVmean ratio combined with SUVmax ratio of ≥ 0.759 identified as the best cut-off value to determine LoVo tumor from LS174T tumor. Our results were in line with the available published reference, as recently research showed that the contrast-to-noise (CNR) indexes of the Gd-RGD tracers in MRI was suitable for differentiating hepatocellular carcinoma (HCC) tissues with high metastatic potential from those with low metastatic potential[28]. However, the present study also had its limitation due to only two kinds of CRC cell lines with different metastatic potentials included in the comparative study. In the future, we will compare the predict potential of ^{18}F-RGD on various types of CRC cell with different metastatic potential.

In conclusion, we firstly investigated the correlation between the tumor makers VEGF/Ki67 expression and ^{18}F-RGD uptake, and the results suggested that ^{18}F-RGD is a promising tracer for tumor imaging and monitoring angiogenesis microenvironment in CRC xenograft mice model. SUVmean ratio of ^{18}F-RGD in PET imaging can be used for differentiating LoVo tumor with high metastatic potential from LS174T tumor with low metastatic potential. Therefore, SUVmean ratio of ^{18}F-RGD is a suitable parameter for predicting the metastatic potential of CRC in animal models.

Abbreviations

CRC
Colorectal carcinoma
CLM
colorectal liver metastases
VEGF
Vascular endothelial growth factor
PET
Positron emission tomography
18F-RGD
18F-AlF-NOTA-E[PEG4-c(RGDfk)]2

Declarations

Authors' contributions

ZMY, JHJ, ZRJ and WZC contributed to conception and design; ZMY, JHJ, ZRJ, JH and WZC contributed to acquisition of data, or analysis and interpretation of data; ZMY, JHJ, JH, and WZC have been involved in drafting the manuscript or revising it critically for important intellectual content; all authors have given final approval of the version to be published.

Acknowledgments

Not applicable

Competing interests

All the authors declare that they have no conflict of interest.

Availability of data and materials

The datasets used and/or analyzed during the current study are available from the corresponding author on reasonable request.

Consent for publication

Not applicable

Ethics approval and consent to participate

All animal experiments were conducted in compliance with the protocols approved by the Institutional Animal Care and Use Committee (IACUC) of Jiangsu Institute of Nuclear Medicine

Funding

This study was supported by grants from the National Key Research and Development Program of China (2019YFC0118100) ; National Natural Science Foundation of China (81671760, 81873910 and 61931013), Scientific Research Transformation Special Fund of Heilongjiang Academy of Medical Sciences□2018415□□Scientific Research Project of Health and Family Planning Commission of Heilong jiang Province(201812 and 201622)□No. [2015] 160 from Beijing Scholars Program.

References

1. Lam VW, Laurence JM, Pang T, Johnston E, Hollands MJ, Pleass HC, Richardson AJ. A systematic review of a liver-first approach in patients with colorectal cancer and synchronous colorectal liver metastases. HPB (Oxford). 2014;16(2):101–8.
2. Torre LA, Bray F, Siegel RL, Ferlay J, Lortet-Tieulent J, Jemal A. Global cancer statistics, 2012. CA Cancer J Clin. 2015;65(2):87–108.
3. Valastyan S, Weinberg RA. Tumor metastasis: molecular insights and evolving paradigms. Cell. 2011;147(2):275–92.
4. Wan L, Pantel K, Kang Y. Tumor metastasis: moving new biological insights into the clinic. Nature medicine. 2013;19(11):1450–64.
5. Ferrara N, Kerbel RS. Angiogenesis as a therapeutic target. Nature. 2005;438(7070):967–74.

6. Wilson PM, LaBonte MJ, Lenz H-J. Assessing the in vivo efficacy of biologic antiangiogenic therapies. Cancer Chemother Pharmacol. 2013;71:1–12.
7. Xu H, Zhang Y, Pena MM, Pirisi L, Creek KE. Six1 promotes colorectal cancer growth and metastasis by stimulating angiogenesis and recruiting tumor-associated macrophages. Carcinogenesis. 2017;38(3):281–92.
8. Lee SH, Jeong D, Han YS, Baek MJ. Pivotal role of vascular endothelial growth factor pathway in tumor angiogenesis. Ann Surg Treat Res. 2015;89(1):1–8.
9. Danhier F, Le Breton A, Preat V. RGD-based strategies to target alpha(v) beta(3) integrin in cancer therapy and diagnosis. Mol Pharm. 2012;9(11):2961–73.
10. Zanella S, Mingozzi M, Dal Corso A, Fanelli R, Arosio D, Cosentino M, Schembri L, Marino F, De Zotti M, Formaggio F, et al. Synthesis, Characterization, and Biological Evaluation of a Dual-Action Ligand Targeting alphavbeta3 Integrin and VEGF Receptors. ChemistryOpen. 2015;4(5):633–41.
11. Yu C, Pan D, Mi B, Xu Y, Lang L, Niu G, Yang M, Wan W, Chen X. (18)F-Alfatide II PET/CT in healthy human volunteers and patients with brain metastases. Eur J Nucl Med Mol Imaging. 2015;42(13):2021–8.
12. Lang L, Ma Y, Kiesewetter DO, Chen X. Stability Analysis of Glutamic Acid Linked Peptides Coupled to NOTA through Different Chemical Linkages. Mol Pharm. 2014;11(11):3867–74.
13. Ding Z, Yang L, Xie X, Xie F, Pan F, Li J, He J, Liang H. Expression and significance of hypoxia-inducible factor-1 alpha and MDR1/P-glycoprotein in human colon carcinoma tissue and cells. J Cancer Res Clin Oncol. 2010;136(11):1697–707.
14. Manfredi S, Lepage C, Hatem C, Coatmeur O, Faivre J, Bouvier AM. Epidemiology and management of liver metastases from colorectal cancer. Ann Surg. 2006;244(2):254–9.
15. Folkman J. Role of angiogenesis in tumor growth and metastasis. Seminars in oncology. 2002;29(6 Suppl 16):15–8.
16. SWITALA-JELEN K, DABROWSKA K, OPOLSKI A, LIPINSKA L, NOWACZYK M. GORSKI A: The Biological Functions of β3 Integrins. Folia Biol (Praha). 2004;50:143–52.
17. Brooks PC, Montgomery AM, Rosenfeld M, Reisfeld RA, Hu T, Klier G, Cheresh DA. Integrin alpha v beta 3 antagonists promote tumor regression by inducing apoptosis of angiogenic blood vessels. Cell. 1994;79(7):1157–64.
18. Cai W, Chen X. Multimodality molecular imaging of tumor angiogenesis. J Nucl Med. 2008;49(Suppl 2):113S–128S.
19. Zhang M, Jiang H, Zhang R, Xu H, Jiang H, Pan W, Li X, Wang Y, Wang S. Noninvasive evaluation of (18)F-FDG/(18)F-FMISO-based Micro PET in monitoring hepatic metastasis of colorectal cancer. Sci Rep. 2018;8(1):17832.
20. Hynes RO. Integrins: Bidirectional,Allosteric Signaling Machines. Cell. 2002;110:673–87.
21. Avraamides CJ, Garmy-Susini B, Varner JA. Integrins in angiogenesis and lymphangiogenesis. Nat Rev Cancer. 2008;8(8):604–17.

22. Bergers G, Benjamin LE. Tumorigenesis and the angiogenic switch. Nat Rev Cancer. 2003;3(6):401–10.
23. Fu X, Yang Y, Li X, Lai H, Huang Y, He L, Zheng W, Chen T. RGD peptide-conjugated selenium nanoparticles: antiangiogenesis by suppressing VEGF-VEGFR2-ERK/AKT pathway. Nanomedicine. 2016;12(6):1627–39.
24. Takagi M, Natsume T, Kanemaki MT, Imamoto N. Perichromosomal protein Ki67 supports mitotic chromosome architecture. Genes Cells. 2016;21(10):1113–24.
25. Yang G, Nie P, Kong Y, Sun H, Hou G, Han J. MicroPET imaging of tumor angiogenesis and monitoring on antiangiogenic therapy with an (18)F labeled RGD-based probe in SKOV-3 xenograft-bearing mice. Tumour Biol. 2015;36(5):3285–91.
26. Li L, Ma L, Shang D, Liu Z, Yu Q, Wang S, Teng X, Zhang Q, Hu X, Zhao W, et al. Pretreatment PET/CT imaging of angiogenesis based on (18)F-RGD tracer uptake may predict antiangiogenic response. Eur J Nucl Med Mol Imaging. 2019;46(4):940–7.
27. Isal S, Pierson J, Imbert L, Clement A, Collet C, Pinel S, Veran N, Reinhard A, Poussier S, Gauchotte G, et al. PET imaging of (68)Ga-NODAGA-RGD, as compared with (18)F-fluorodeoxyglucose, in experimental rodent models of engrafted glioblastoma. EJNMMI Res. 2018;8(1):51.
28. Li TR, Yu MH, Huang XB, Yang ZJ, Lu GM, Li YJ. Magnetic Resonance Gd-RGD Imaging Study of Hepatocellular Carcinoma with High and Low Metastatic Potential before and after Human Bone Marrow-derived Mesenchymal Stem Cell Intervention. Chin Med J (Engl). 2017;130(21):2591–600.

Figures

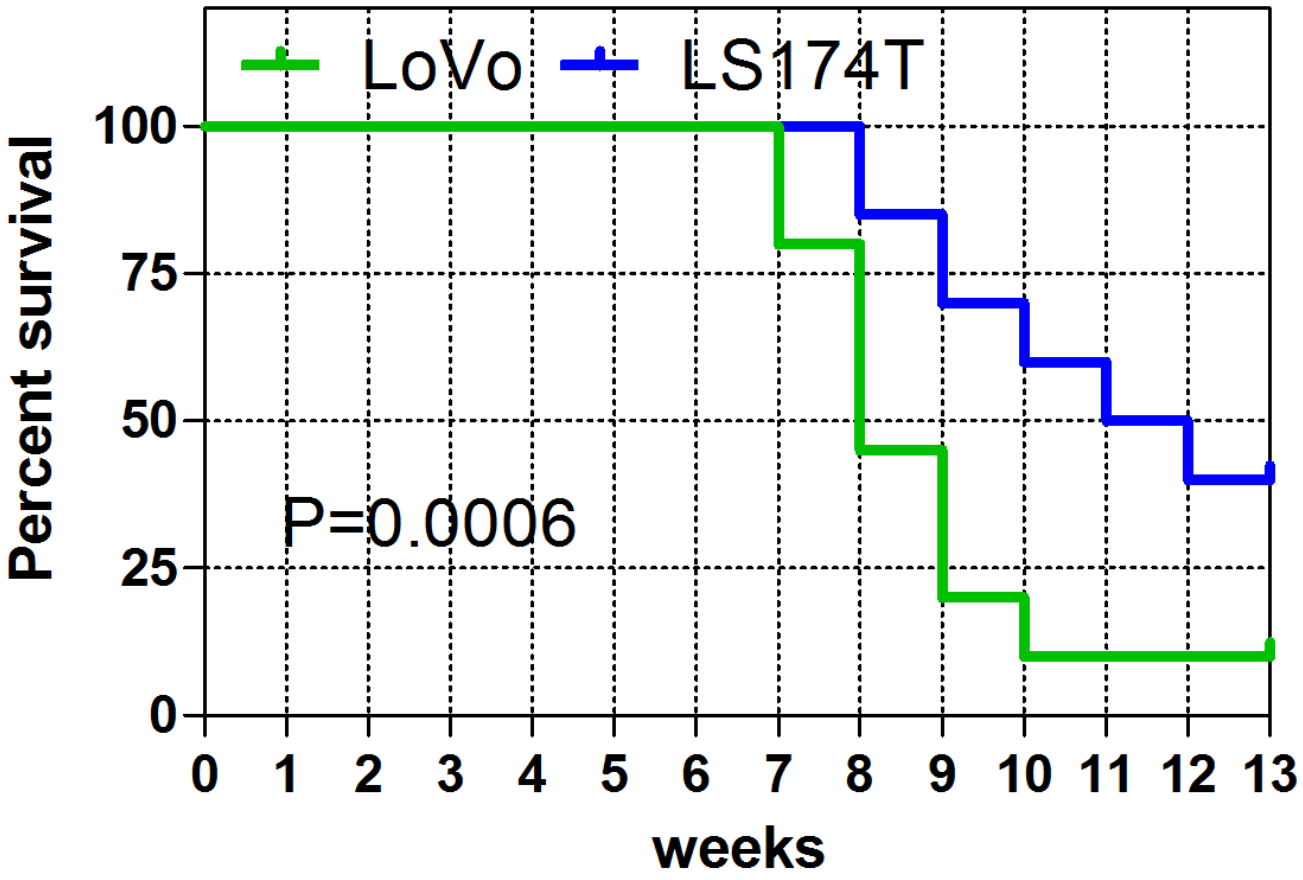

Figure 1

Survival analysis of LoVo and LS174T liver metastasis model. n=20.

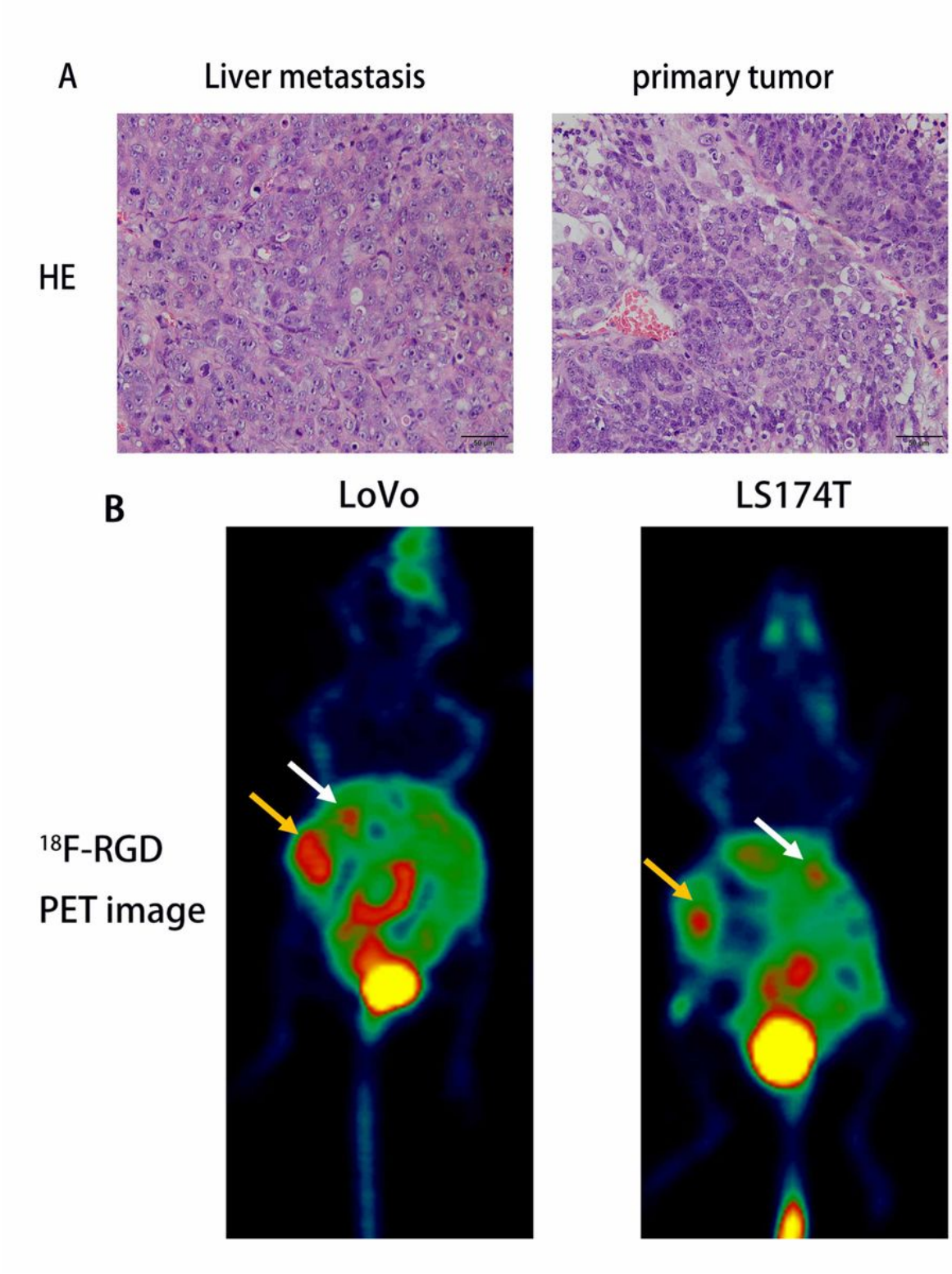

Figure 2

In vivo whole-body Micro-PET images of 18F-RGD. A: HE staining of liver metastasis tumor and primary tumor. B: White arrows indicate the uptake of 18F-RGD in liver metastasis tumor. Yellow arrows indicate the uptake of 18F-RGD of the primary tumor in spleen.

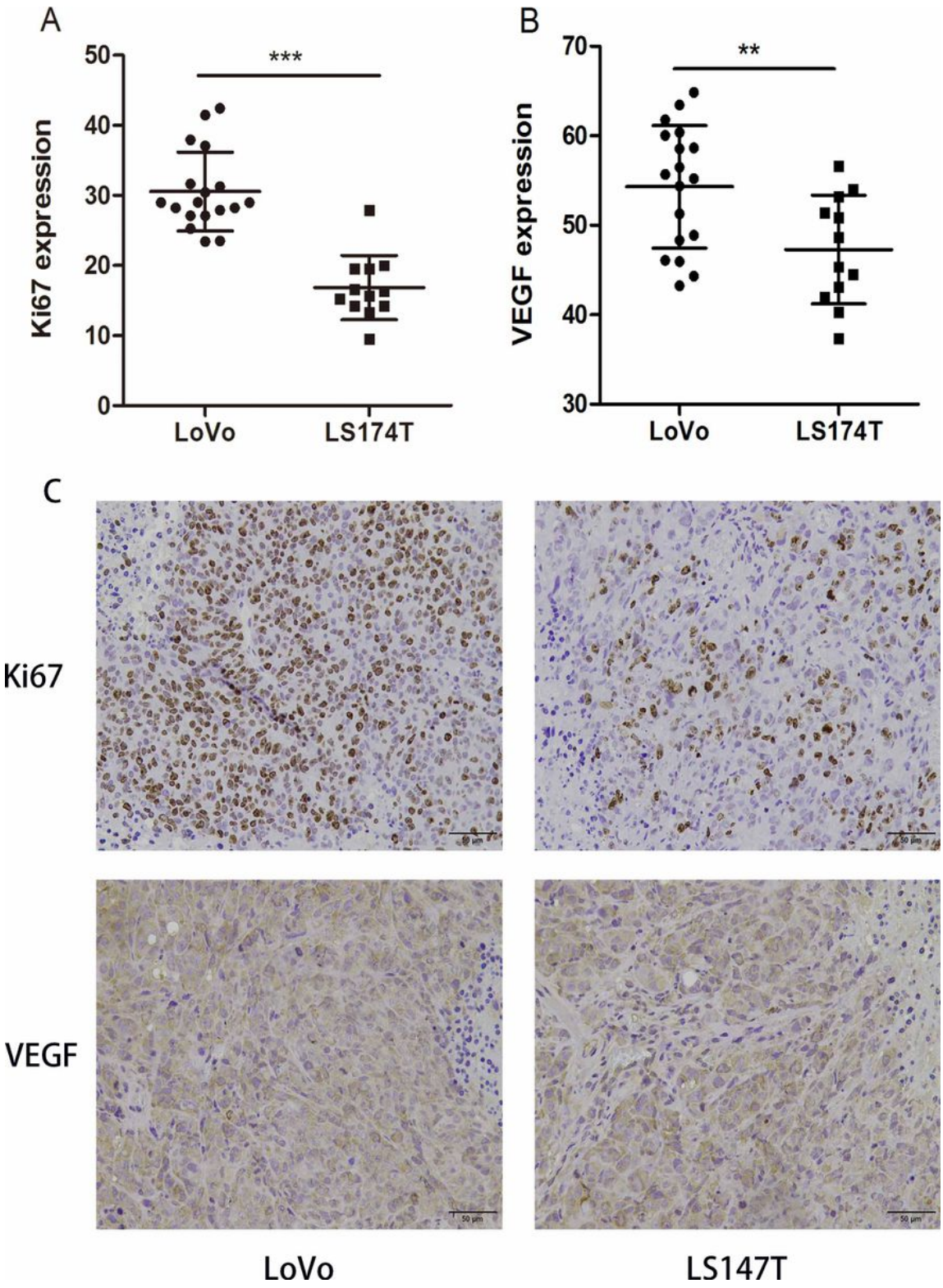

Figure 3

Comparison of Ki67 and VEGF expression protein between LoVo and LS174T primary tumors. A: Immunohistochemical staining for Ki67/VEGF (brown) in LoVo (left side) and LS174T (right side) primary tumor tissues (magnification, 200×), respectively. B: Quantification of Ki67 (left) and VEGF (right) from immunohistochemical staining. ***P□0.0001, **P□0.001.

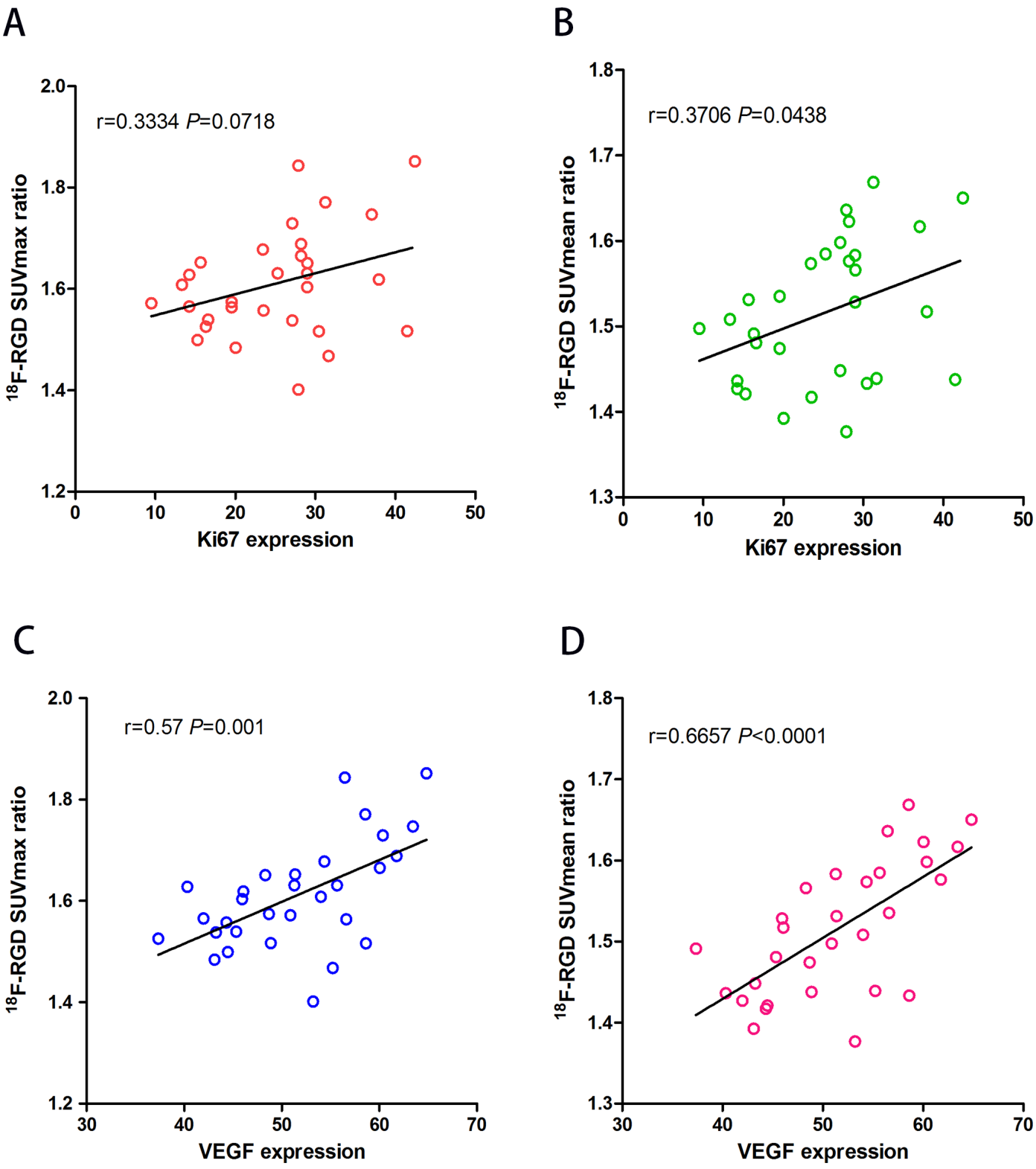

Figure 4

Correlation analysis between RGD parameters and biomarkers. A: correlation of 18F-RGD SUVmax ratio between Ki67 expression. B: correlation of 18F-RGD SUVmean ratio between Ki67 expression. C: correlation of 18F-RGD SUVmax ratio between VEGF expression. D: correlation of 18F-RGD SUVmean ratio between VEGF expression.

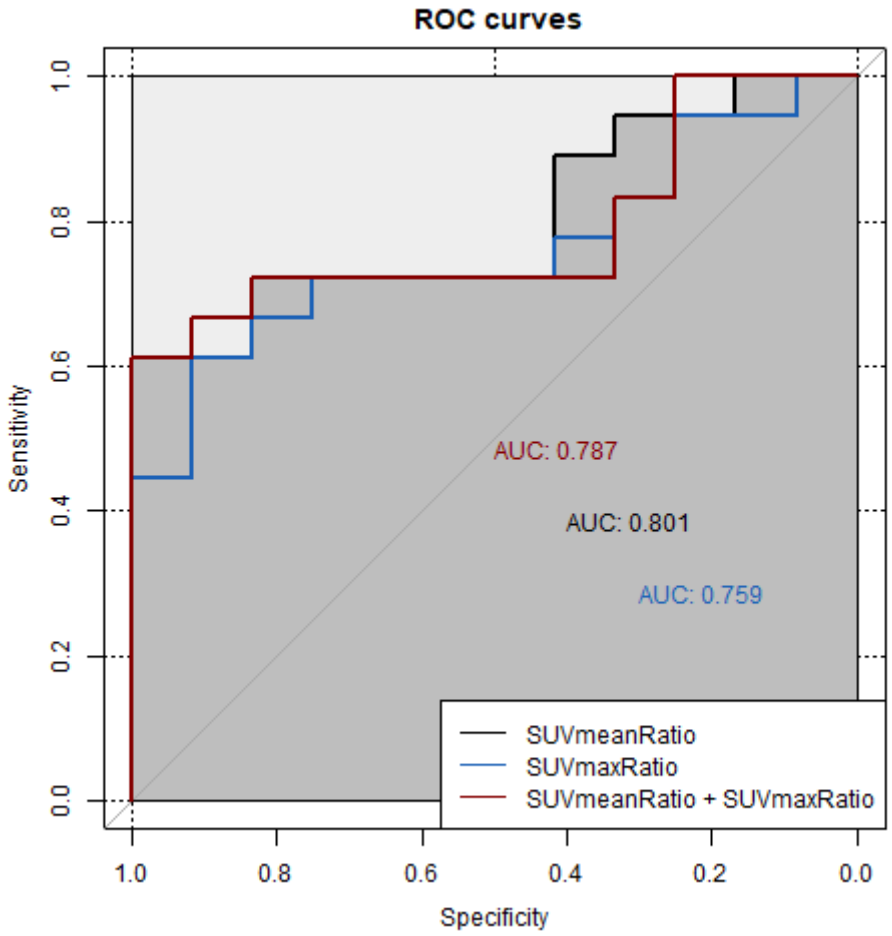

Figure 5

ROC curves analysis of different RGD parameters to distinguish LoVo tumor from LS174T tumor.